

Interaction between two neighboring tunnel using PFC2D

V. Sarfarazi¹, Hadi Haeri^{*2}, Salman Safavi², Mohammad Fatehi Marji³ and Zheming Zhu⁴

¹Department of Mining Engineering, Hamedan University of Technology, Hamedan, Iran

²Department of Civil Engineering, Malard Branch, Islamic Azad University, Malard, Iran

³Mine Exploitation Engineering Department, Faculty of Mining and Metallurgy, Institution of Engineering, Yazd University, Yazd, Iran

⁴MOE Key Laboratory of Deep Underground Science and Engineering, School of Architecture and Environment, Sichuan University, Chengdu 610065, China

(Received January 28, 2019, Revised March 16, 2019, Accepted March 20, 2019)

Abstract. In this paper, the interaction between two neighboring tunnel has been investigated using PFC2D. For this purpose, firstly calibration of PFC was performed using Brazilian experimental test. Secondly, various configuration of two neighboring tunnel was prepared and tested by biaxial test. The maximum and minimum principle stresses were 0.2 and 30 MPa respectively. The modeling results show that in most cases, the tensile cracks are dominant mode of cracks that occurred in the model. With increasing the diameter of internal circle, number of cracks decreases in rock pillar also number of total cracks decreases in the model. The rock pillar was heavily broken when its width was too small. In fixed quarter size of tunnel, the crack initiation stress decreases with increasing the central tunnel diameter. In fixed central tunnel size, the crack initiation stress decreases with increasing the quarter size of tunnel.

Keywords: PFC2D, tunnel, tensile crack

1. Introduction

Tunnel excavation will cause the re-adjustment of existing stress fields in surrounding rock masses. Therefore, the excavation of a tunnel near an existing tunnel will also cause the re-adjustment of stress fields around the first tunnel, which has been stabilized with the help of a support system. The re-adjustment of the stress field will cause further changes in the support loads and deformation of the existing tunnel. Many attempts are made to investigate tensile and compressive failure modes of rock materials (Sarfarazi and Haeri 2016, Haeri *et al.* 2016a,b). The interaction process in between adjacent tunnels have been studied by many researchers (Ghaboussi and Ranken 1977, Kovári 2003, Shin *et al.* 2005, Liu *et al.* 2009, Xie *et al.* 2004, Gerçek 2005, Chehade and Shahrour 2008, Kim and Bae 2008, Hsiao *et al.* 2009, Kim *et al.* 2012, Chen *et al.* 2011 and Li and Yuan 2012, Kim and Lee 2013, Huang *et al.* 2012, Ramadoss 2013, Chung *et al.* 2013, Kang *et al.* 2014, Jung *et al.* 2014, Ye *et al.* 2014, Nejati and Ghazvinian 2014, Lim and Son 2014, Pan 2014, Panaghi *et al.* 2015, Zhao 2015, Kequan 2015, Li *et al.* 2015, Shi *et al.* 2015, Haeri and Sarfarazi 2016, Kim and Kim 2017, Das *et al.* 2017, Nabil *et al.* 2017, Monfared 2017, Boumaaza *et al.* 2017, Rooh *et al.* 2018, Khodayar and Nejati 2018). However, several classical numerical approaches have been devoted to study the stresses and displacement fields around the two neighboring tunnels under different loading and geometrical conditions. The finite element, finite difference

boundary element methods or a combination of these numerical methods have been developed and used by several researches. for the stability analyses of surface and underground rock structures (Marji *et al.* 2008, Siahmansouri *et al.* 2012).

Many numerical methods can be applied to investigate interaction between two neighboring tunnel, such as General Particle Dynamics (GPD), Peridynamics(PD), The Extended Finite Element Method.

A series of finite element analyses is performed by Ghaboussi and Ranken (1977) to investigate the mechanical behavior of systems of two parallel and neighboring tunnels. They considered various situations related to the excavation sequences and support installation process of these two tunnels. Stability analyses of two parallel circular tunnels considering different tunnel diameters in a cohesive soil were accomplished by Xie *et al.* (2004). They used the finite element method (FEM) and theory of plasticity to investigate the relationship between the pillar width (the distance separating the two neighboring parallel tunnels) and the collapsing ratio.

Chehade and Shahrour (2008) performed a parametric study on twin tunnels using FEM to examine the effect of the relative position of tunnels (i.e. considering the horizontal, vertical or inclined alignment of the twin tunnels). They also considered the construction process based on the soil movements and internal forces in the tunnel lining. They found that the vertical tunnel alignment gives the maximum soil settlement while the horizontal alignment may give the minimum amount of settlement.

Haeri *et al.* 2018, investigated the effect of particle size on the single edge-notched rectangle bar in bending test using PFC3D simulation. Also, Haeri *et al.* 2018 studied the

*Corresponding author, Assistant Professor
E-mail: haerihadi@gmail.com

effect of ball size on the hollow center cracked disc (HCCD) in Brazilian test.

Kang *et al.* (2014) studied the behavior of rock pillar in the diverging area of road tunnel by a three dimensional numerical simulation and proposed a safety factor chart to reflect the effects of pillar width, tunnel overburden depth, and rock condition. On the other hand, Kim and Bae (2008) performed a series of scaled model test on three parallel tunnels and, by examining crack initiating pressures and deformation behaviors, investigated their stability including the effects of pillar widths, tunnel sectional shapes, supports and ground conditions. Concerning the interaction between adjacent tunnels, however, most studies have been focused on parallel tunnels as described and, moreover, many cases of which were for circular tunnels or for tunnels in symmetric conditions. Little attention has been paid to the interaction between two tunnels in asymmetric geometric configurations. This study concerns the interaction between two asymmetric circular tunnels.

2. Numerical simulation with discrete element method

Discrete element method (DEM) can also be effectively used for the stability analyses of twin tunnels under various conditions. The two dimensional particle flow code (PFC2D) which is a sophisticated computer software developed by Itasca 1999 (version 3.1 and later on modified by Potyondy and Cundall, 2004) has been used in this research for the stability analyses of two parallel adjacent tunnels.

2.1 Numerical modeling by PFC2D based on the bonded particle model approach

The two dimensional particle flow code (PFC2D) is versatile discrete element software used to solve many geo-mechanical problems used in various fields of rock engineering. The version 3.1 of Itasca 1999 modified by Potyondy and Cundall (2004) is used in this research to represent the rock material as an assembly of rigid particles. These particles can move independently within the assembly and are interact one another at the contact points. An explicit central finite difference scheme is applied to this DEM code to model the particles movements and the interaction forces by adopting both the linear and non-linear contact models. This modeling technique also taking into account the frictional sliding in between the particles within the assembly. In the present study, it is required to provide an elastic relationship in between the contact forces and the relative movements of the particles by using the linear contact model in PFC2D. Therefore, a parallel-bond particle model is adopted using the following micro-mechanical properties within the particle assembly model: i) the stiffness ration K_n over K_s , ii) the friction coefficient and the contact modulus of the ball-to-ball contact points, iii) the parallel normal and shear bonding stresses, iv) the radius of the typical ball, v) the radius multiplier, modulus and stiffness ration for parallel-bond contacts and vi) the ratio of standard deviation to that of the mean normal and

shear bonding strengths. The suitable micromechanical properties required to model the particle assembly can be established by using the standard calibration process adopted in PFC2D. The laboratory measured macro-mechanical properties of natural material cannot be directly used to represent the corresponding micro-mechanical properties needed for numerical simulation of the material sample in a standard DEM code. The macro-mechanical properties reflect the continuum behavior of testing samples, therefore, an inverse modeling technique is adopted in Itasca 1999 version 3.1 software to estimate the appropriate micro-mechanical properties for the particle assembly model. This is a trial- and-error algorithm relating these two sets of the material properties as suggested by Itasca 1999. This algorithm assumes the micro mechanical properties for a particular particle assembly and compares the deformation and strength characteristics of the models with those of the laboratory specimens. The suitable micro-mechanical properties which give simulated macro mechanical values close to those measured from the laboratory tests can be adopted to be used for modeling the discontinuous rock masses containing joints. The limitations of DEM are as follow: (a) Fracture is closely related to the size of elements, and that is so called size effect. (b) Cross effect exists because of the difference between the size and shape of elements with real grains. (c) In order to establish the relationship between the local and macroscopic constitutive laws, data obtained from classical geomechanical tests which may be impractical are used (Donze FV, Richefeu V, Magnier SA (2009)).

2.2 Calibrating the numerical model for the problem

The two standard uniaxial compression and Brazilian tensile strength tests were used to calibrate the testing specimen or model in PFC2D. The particle assembly model is generated by the modeling software considering the following four steps: i) generating and packing the particles for the particle assembly model, ii) installing the isotropic stress situation, iii) eliminating the floating particles and iv) installing the bonds in between the particles with in the assembly. Table 1 gives the micro-properties adopted in this modeling technics based on the calibration process provided by Potyondy and Cundall, 2003. These properties can be used to generate a calibrated particle assembly in PFC2D. In this calibration process the diameter of the Brazilian disc samples is taken as 54 mm. The testing sample is made of 5,615 particles in the particle assembly model. During the loading process, a suitable speed of 0.016 m/s is adopted in this modeling procedure to crush the lateral walls of the disc toward each other. The failure process of the testing samples are illustrated in Figures 1a and 1b. The distribution of particles displacement vectors and bonding forces are shown in Fig. 2. This figure shows the failure planes in the corresponding laboratory and numerical tests are well matching. Table 2 compares the experimental and numerical strengths of the testing samples and show a good agreement in between the corresponding numerical and experimental strength values.

Fig 3 shows numerical compression test results. Red line and black line shows shear crack and tensile cracks,

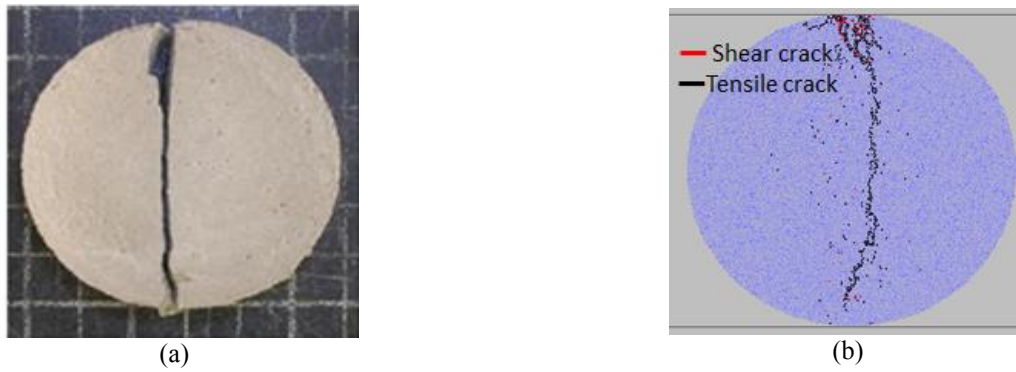


Fig. 1 failure pattern in a) physical sample, b) PFC2D model

Table 1 Micro properties used to represent the intact rock

Parameter	Value	Parameter	Value
Type of particle	disc	Parallel bond radius multiplier	1
density	3000	Young modulus of parallel bond (GPa)	40
Minimum radius	0.27	Parallel bond stiffness ratio	1.7
Size ratio	1.56	Particle friction coefficient	0.4
Porosity ratio	0.08	Parallel bond normal strength, mean (MPa)	30
Damping coefficient	0.7	Parallel bond normal strength, SD (MPa)	2
Contact young modulus (GPa)	40	Parallel bond shear strength, mean (MPa)	30
Stiffness ratio	1.7	Parallel bond shear strength, SD (MPa)	2

Table 2 Brazilian tensile strength of physical and numerical samples

Physical tensile strength (MPa)	4.5 and 4.7
Numerical tensile strength (MPa)	4.5

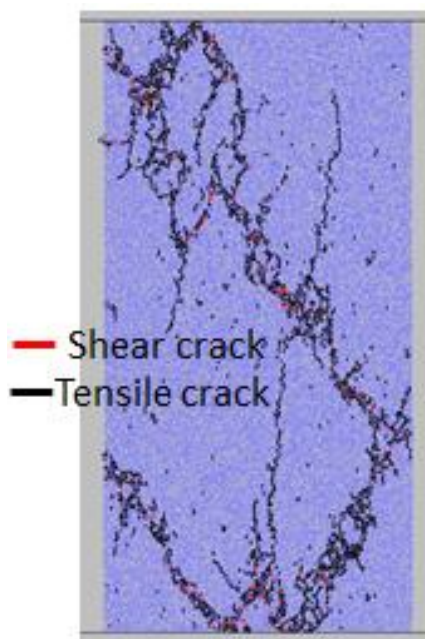


Fig. 2 Numerical compression test result

respectively. As can be seen tensile cracks develop within the model. This is accordance to typical failure pattern occurred in experimental test.

2.3 model preparation of the problem using Particle Flow Code

Finishing the calibration process of the PFC2D, a rectangular model is created in the code to simulate the biaxial compression testing samples with the dimension of 70*70 mm. Rectangular models are consisted of one quarter of circular tunnel and a circle tunnel that situated at center of the model. The radius of one quarter of circular tunnel was 10 mm (Fig 3), 15mm (Fig 4) and 20mm (Fig 5). The radius of central tunnel were 5mm, 10mm, 15mm, 20mm and 25mm. These models are loaded biaxially (Fig 3, 4 and 5). The values of minimum and maximum principal stress was registered at 0.2 MPa and 30 MPa, respectively. The compressive force was registered by taking the reaction forces on the upper wall.

3. Numerical results

3.1 Failure pattern in numerical models

a) The radius of one quarter of circular tunnel is 10 mm

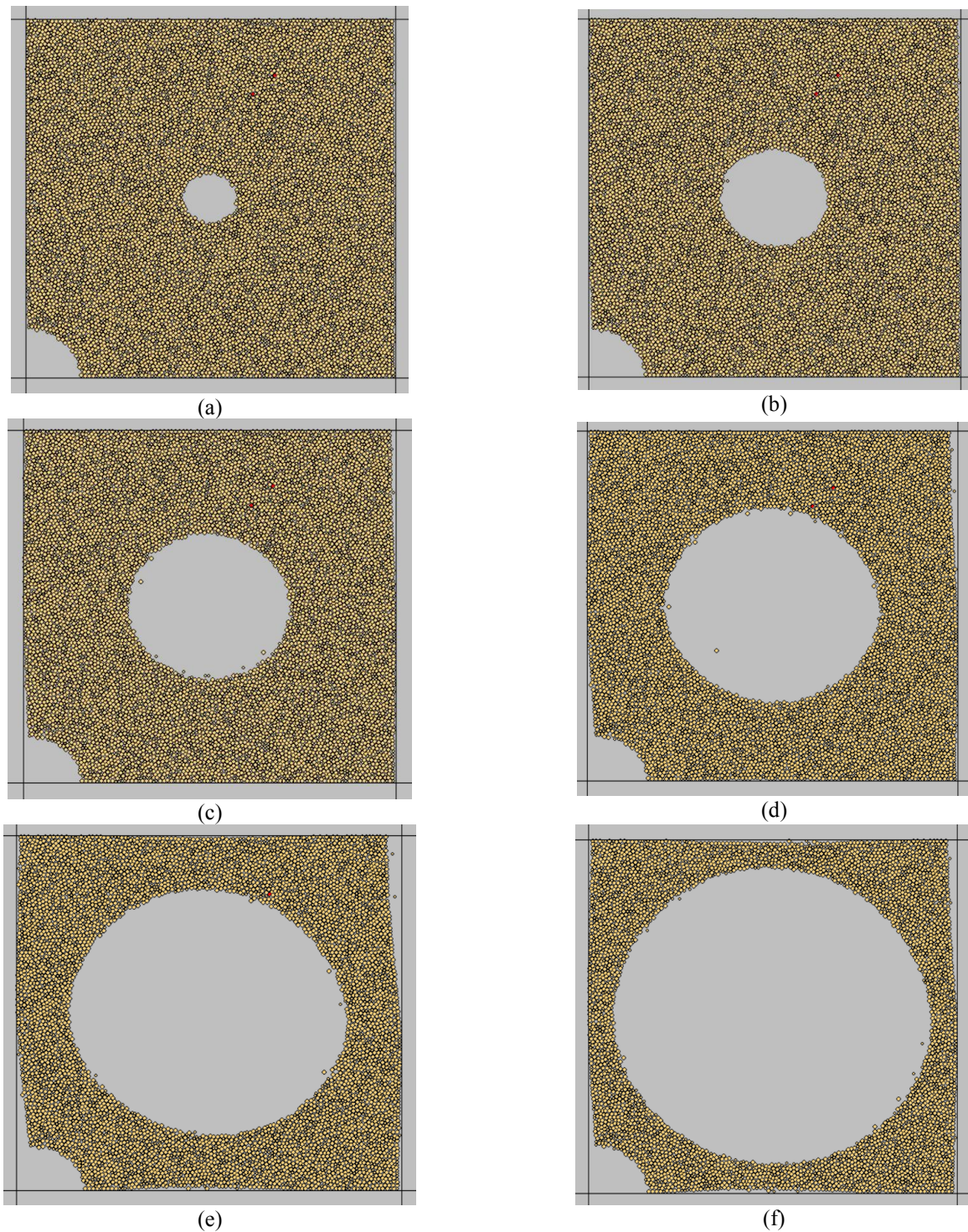


Fig 3. The radius of one quarter of circular tunnel is 10 mm while diameter of central tunnel were a)5mm, b)10mm, c)15mm, d)20 mm, e)25 mm and f)30 mm

Fig 6 shows failure pattern in numerical models. Red line and black line is representative of shear crack and tensile crack, respectively.

A-1-Diameter of internal circle was 5 mm:

When diameter of internal circle was 5mm (Fig 6a), tensile cracks initiate in rock pillar between two cavities.

Also, three tensile joint set initiate near the central hole and propagates diagonally till coalescence with model boundary.

A-2-Diameter of internal circle was 10 mm:

When diameter of internal circle was 10mm (Fig 6b), tensile cracks initiate in rock pillar between two cavities. Also, three tensile joint set initiate near the central hole and propagates diagonally till coalescence with model boundary.

A-3-Diameter of internal circle was 15 mm:

When diameter of internal circle was 15 mm(Fig 6c), tensile cracks initiate in rock pillar between two cavities.

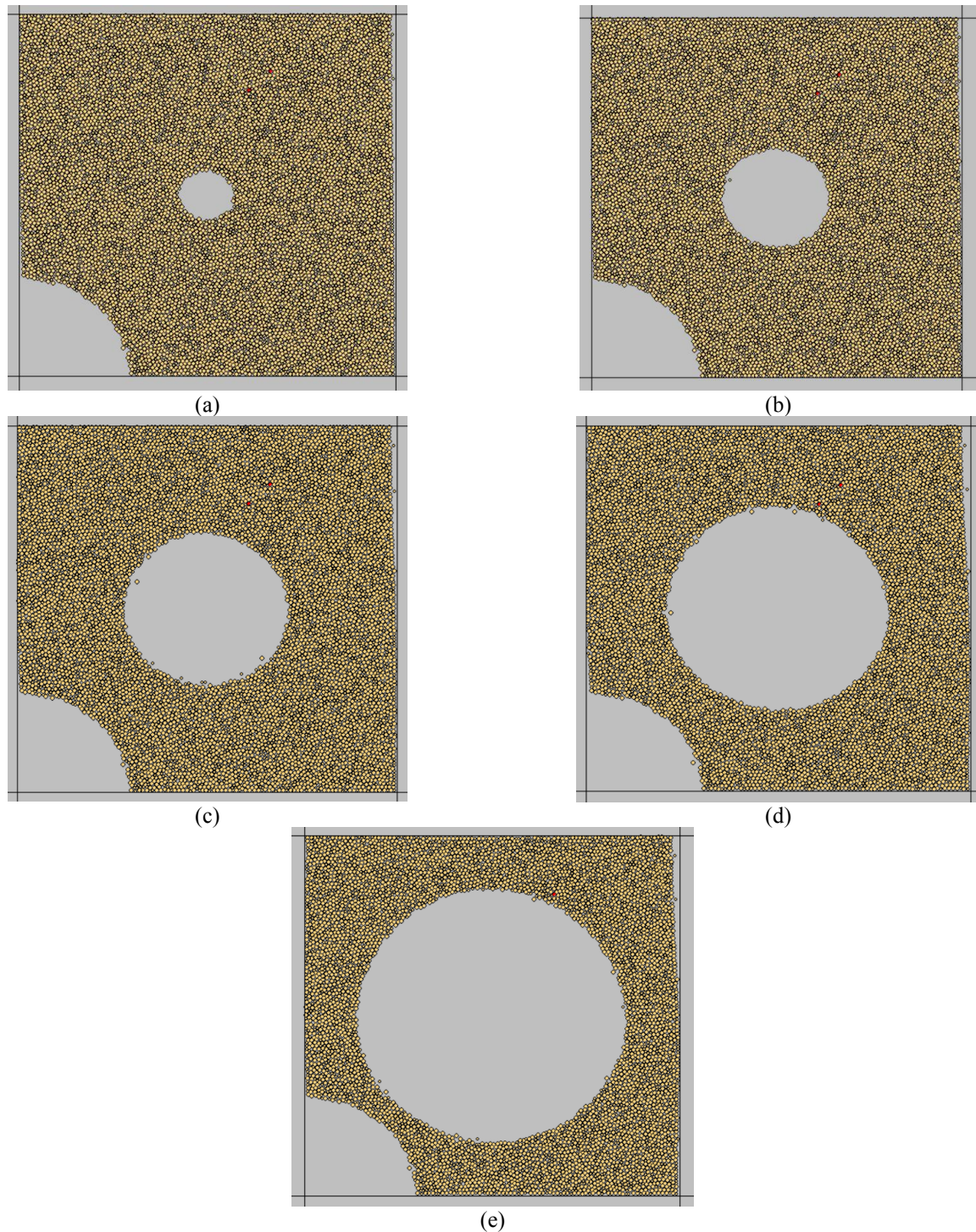


Fig 4. The radius of one quarter of circular tunnel is 15 mm while diameter of central tunnel were a)5mm, b)10mm, c)15mm, d)20 mm, e)25 mm

Also, three tensile joint set initiate near the central hole and propagates diagonally till coalescence with model boundary.

A-4-Diameter of internal circle was 20 mm:

When diameter of internal circle was 20 mm(Fig 6d), tensile cracks initiate in rock pillar between two cavities. Also, three tensile joint set initiate near the central hole and propagates diagonally till coalescence with model boundary.

A-5-Diameter of internal circle was 25 mm:

When diameter of internal circle was 25 mm (Fig 6e), tensile cracks initiate in rock pillar between two cavities. Also, two tensile joint set initiate near the central hole and propagates diagonally till coalescence with model boundary.

A-6-Diameter of internal circle was 30 mm:

When diameter of internal circle was 30mm (Fig 6f), tensile cracks initiate in vertical rock pillar.

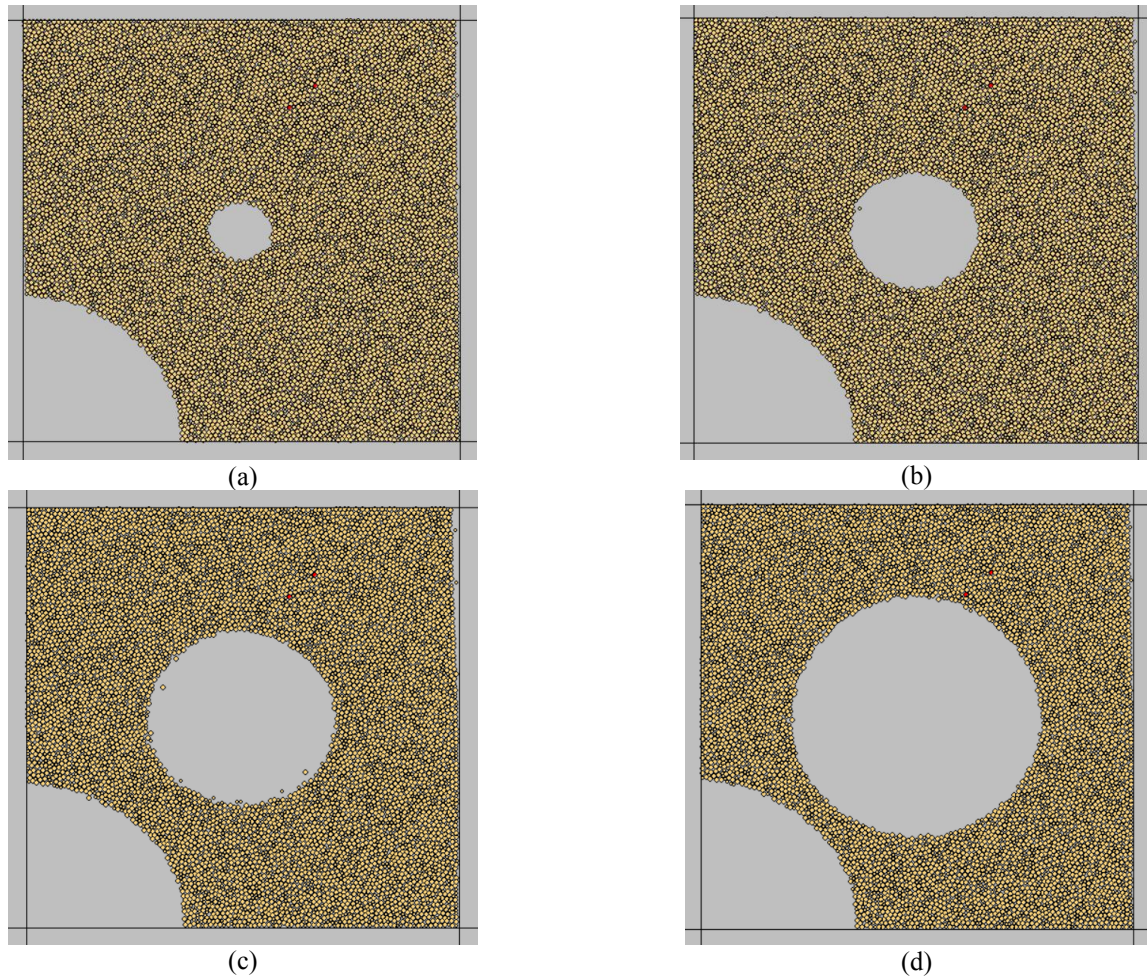


Fig 5. The radius of one quarter of circular tunnel is 20 mm while diameter of central tunnel were a)5mm, b)10mm, c)15mm, d)20 mm

From above finding it can be concluded that with increasing the diameter of internal circle, number of cracks decreases in rock pillar also number of total cracks decreases in the model.

b) The radius of one quarter of circular tunnel is 15 mm

Fig 7 shows failure pattern in numerical models. Red line and black line are representative of shear crack and tensile crack, respectively.

B-1-Diameter of internal circle was 5 mm:

When diameter of internal circle was 5mm (Fig 7a), tensile cracks initiate in rock pillar between two cavities. Also, three tensile joint set initiate near the central hole and propagates diagonally till coalescence with model boundary.

B-2-Diameter of internal circle was 10 mm:

When diameter of internal circle was 10mm (Fig 7b), tensile cracks initiate in rock pillar between two cavities.

Also, two tensile joint set initiate near the central hole and propagates diagonally till coalescence with model boundary.

B-3-Diameter of internal circle was 15 mm:

When diameter of internal circle was 15 mm (Fig 7c), tensile cracks initiate in rock pillar between two cavities. Also, two tensile joint set initiate near the central hole and propagates diagonally till coalescence with model

boundary.

B-4-Diameter of internal circle was 20 mm:

When diameter of internal circle was 20 mm (Fig 7d), tensile cracks initiate in rock pillar between two cavities. Also, two tensile joint set initiate near the central hole and propagates diagonally till coalescence with model boundary.

B-5-Diameter of internal circle was 25 mm:

When diameter of internal circle was 25 mm (Fig 7e), tensile cracks initiate in rock pillar between two cavities.

Also, two tensile joint set initiate near the central hole and propagates diagonally till coalescence with model boundary.

c) The radius of one quarter of circular tunnel is 20 mm

Fig 8 shows failure pattern in numerical models. Red line and black line are representative of shear crack and tensile crack, respectively.

C-1-Diameter of internal circle was 5 mm:

When diameter of internal circle was 5mm (Fig 8a), tensile cracks initiate in rock pillar between two cavities.

Also, two tensile joint set initiate near the central hole and propagates diagonally till coalescence with model boundary.

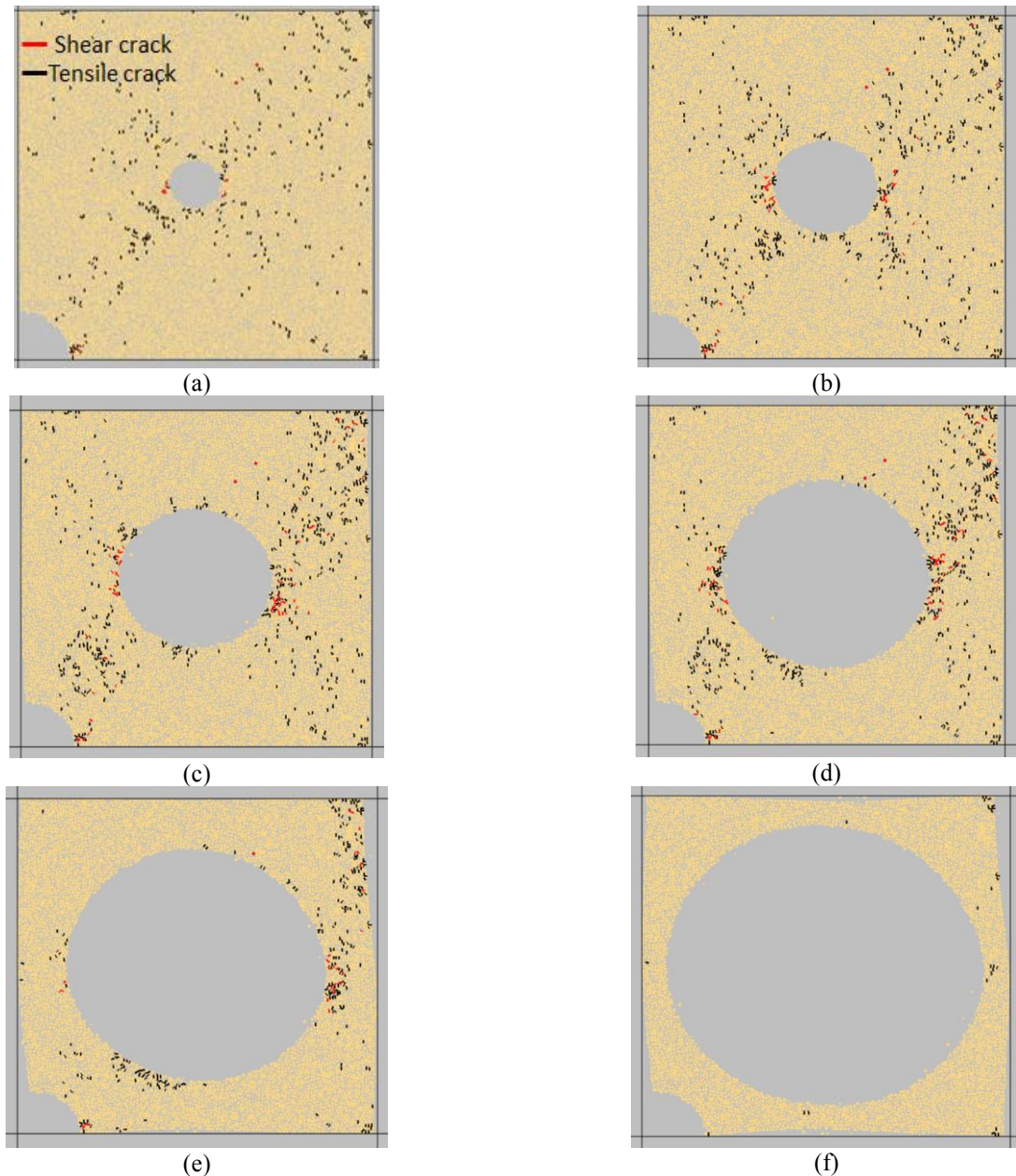


Fig 6. The radius of one quarter of circular tunnel is 10 mm while diameter of central tunnel were a)5 mm, b)10 mm, c)15 mm, d)20 mm, e)25 mm and f)30 mm

C-2-Diameter of internal circle was 10 mm:

When diameter of internal circle was 10mm (Fig 8b), tensile cracks initiate in rock pillar between two cavities. Also, two tensile joint set initiate near the central hole and propagates diagonally till coalescence with model boundary.

C-3-Diameter of internal circle was 15 mm:

When diameter of internal circle was 15 mm (Fig 8c), tensile cracks initiate in rock pillar between two cavities. Also, two tensile joint set initiate near the central hole and propagates diagonally till coalescence with model boundary.

C-4-Diameter of internal circle was 20 mm:

When diameter of internal circle was 20mm (Fig 8d), tensile cracks initiate in rock pillar between two cavities.

From above finding it can be concluded that with increasing the diameter of internal circle, number of cracks decreases in rock pillar also number of total cracks decreases in the model.

c) The radius of one quarter of circular tunnel is 20 mm

Fig 8 shows failure pattern in numerical models. Red line and black line are representative of shear crack and tensile crack, respectively.

C-1-Diameter of internal circle was 5 mm:

When diameter of internal circle was 5mm (Fig 8a), tensile cracks initiate in rock pillar between two cavities.

Also, two tensile joint set initiate near the central hole and propagates diagonally till coalescence with model boundary.

C-2-Diameter of internal circle was 10 mm:

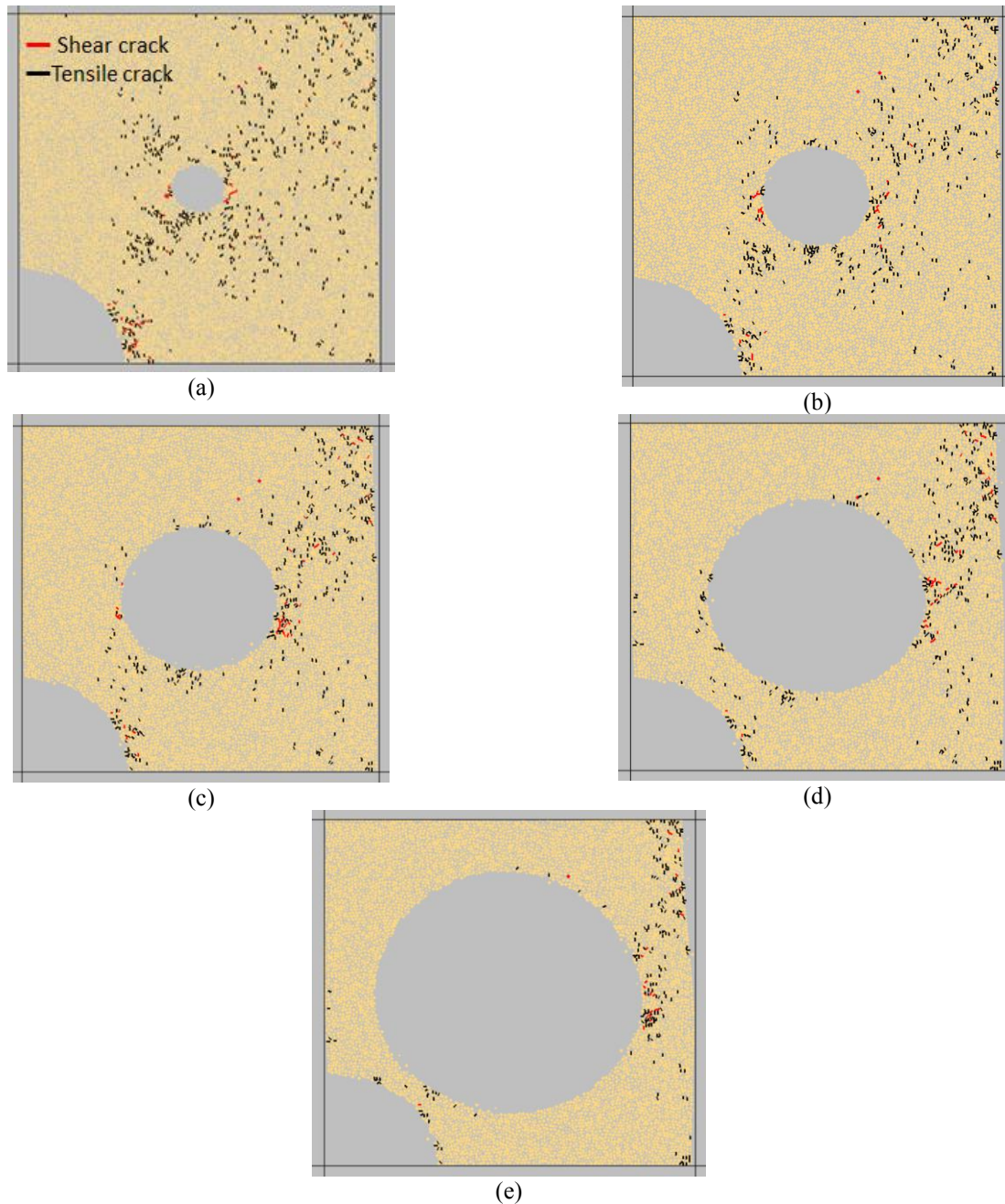


Fig 7. The radius of one quarter of circular tunnel is 15 mm while diameter of central tunnel were a)5mm, b)10mm, c)15mm, d)20 mm, e)25 mm

When diameter of internal circle was 10mm (Fig 8b), tensile cracks initiate in rock pillar between two cavities. Also, two tensile joint set initiate near the central hole and propagates diagonally till coalescence with model boundary

C-3-Diameter of internal circle was 15 mm:

When diameter of internal circle was 15 mm (Fig 8c), tensile cracks initiate in rock pillar between two cavities. Also, two tensile joint set initiate near the central hole and propagates diagonally till coalescence with model boundary.

C-4-Diameter of internal circle was 20 mm:

When diameter of internal circle was 20mm (Fig 8d), tensile cracks initiate in rock pillar between two cavities.

From above finding it can be concluded that with

increasing the diameter of internal circle, number of cracks decreases in rock pillar also number of total cracks decreases in the model.

3.2 The effect of a central tunnel diameter on the crack initiation stress:

Fig 9 shows the effect of diameter of central tunnel on the crack initiation stress.

4. Conclusion

Interaction in between the twin tunnels have been studied by the discrete element method. The main results

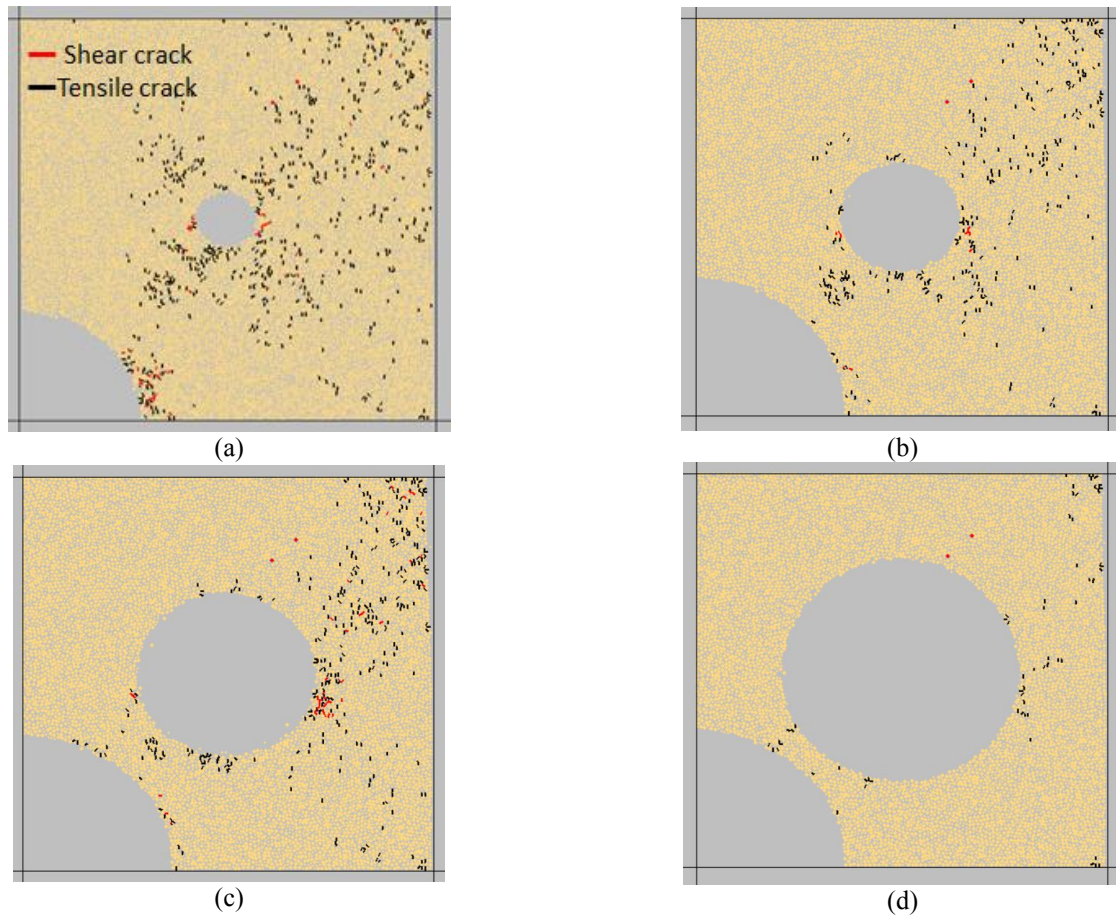


Fig. 8 The radius of one quarter of circular tunnel is 10 mm while diameter of central tunnel were a)5mm, b)10mm, c)15mm, d)20 mm.

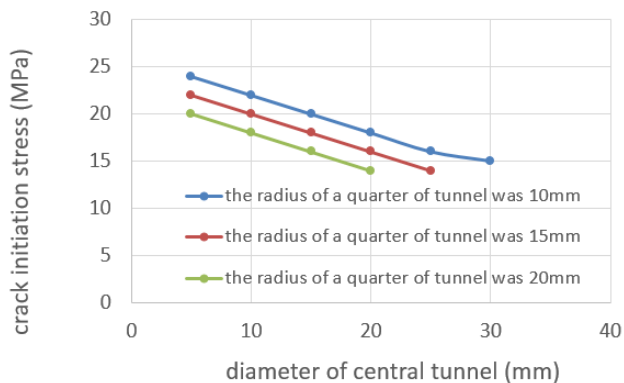


Fig. 9 the effect of diameter of central tunnel on the crack initiation stress.

may be classified as:

- The most dominant induced cracks in the model are those of tensile mode.
- With increasing the diameter of internal circle, number of cracks decreases in rock pillar also number of total cracks decreases in the model. The rock pillar was heavily broken when its width was too small.
- In fixed quarter size of tunnel, the crack initiation stress decrease with increasing the central tunnel diameter.

- In fixed central tunnel size, the crack initiation stress decrease with increasing the quarter size of tunnel.

References

- Boumaaza, M., Bezazi, A., Bouchelaghem, H., Benzennache, N., Amziane, S. and Scarpa, F. (2017), "Behavior of pre-cracked deep beams with composite materials repairs", *Struct. Eng. Mech.*, **63**(4), 43-56.
- Cehade, F.H. and Shahrou, I. (2008), "Numerical analysis of the interaction between twin-tunnels: Influence of the relative position and construction procedure", *Tunn. Undergr. Sp. Tech.*, **23**, 210-214. <https://doi.org/10.1016/j.tust.2007.03.004>.
- Chen, R.P., Zhu, J., Liu, W. and Tang, X.W. (2011), "Ground movement induced by parallel EPB tunnels in silty soils", *Tunnelling and Underground Space Technology*, **26**(1), 163-171. <https://doi.org/10.1016/j.tust.2010.09.004>.
- Chung, J.S., Moon, I.K. and Yoo, C.H. (2013), "Behaviour characteristics of tunnel in the cavity ground by using scale model tests", *J. Korean Geo-Environ. Soc.*, **14**(12), 61-69
- Das, R., Singh, P.K., Kainthoal, A., Panthee, S. and Singh, T.N. (2017), "Numerical analysis of surface subsidence in asymmetric parallel highway tunnels", *J. Rock Mech. Geotech. Eng.*, **9**, 170-179. <https://doi.org/10.1016/j.jrmge.2016.11.009>.
- Donze, F.V., Richefeu, V. and Magnier, S.A. (2009), "Advances in discrete element method applied to soil rock and concrete mechanics", *Electronic J. Geological Eng.*, **8**, 1-44.

- Gerçek, H. (2005), "Interaction between parallel underground openings", *The 19th International Mining Congress and Fair of Turkey*, Izmir, Turkey, June. 73-81.
- Ghaboussi, J. and Ranken, R.E. (1977), "Interaction between two parallel tunnels", *Int. J. Numer. Anal. Met.*, **1**(1), 75-103. <https://doi.org/10.1002/nag.1610010107>.
- Haeri, H., Sarfarazi, V. and Zhu, Z. (2018), "PFC3D simulation of the effect of particle size on the single edge-notched rectangle bar in bending test", *Struct. Eng. Mech.*, **68**(4), 497-505. <http://dx.doi.org/10.12989/sem.2018.68.4.497>.
- Haeri, H., Sarfarazi, V., Zhu, Z. and Moradzadeh, M. (2018), "The effect of ball size on the hollow center cracked disc (HCCD) in Brazilian test", *Comput. Concrete*, **22**(4), 373-381. <http://dx.doi.org/10.12989/cac.2018.22.4.373>.
- Haeri, H., Sarfarazi, V. and Hedayat, A. (2016a), "Suggesting a new testing device for determination of tensile strength of concrete", *Struct. Eng. Mech.*, **60**(6), 939-952. <http://dx.doi.org/10.12989/sem.2016.60.6.939>.
- Haeri, H. and Sarfarazi, V. (2016), "Experimental study of shear behavior of planar non-persistent joint", *Comput. Concrete*, **17**(5), 639-653. <http://doi.org/10.12989/cac.2016.17.5.649>.
- Haeri, H., Sarfarazi, V., Marji, M.F., Hedayat, A. and Zhu, Z. (2016b), "Experimental and numerical study of shear fracture in brittle materials with interference of initial double cracks", *Acta Mechanica Solida Sinica*, **29**(5), 555-566. [https://doi.org/10.1016/S0894-9166\(16\)30273-7](https://doi.org/10.1016/S0894-9166(16)30273-7).
- Hsiao, F.Y., Wang, C.L. and Chern, J.C. (2009), "Numerical simulation of rock deformation for support design in tunnel intersection area", *Tunn. Undergr. Sp. Tech.*, **24**, 14-21. <https://doi.org/10.1016/j.tust.2008.01.003>.
- Huang, X., Huang, H. and Zhang, J. (2012), "Flattening of jointed shield-driven tunnel induced by longitudinal differential settlements", *Tunnel. Underground Space Technol.*, **31**, 20-32. <https://doi.org/10.1016/j.tust.2012.04.002>.
- Itasca Consulting Group Inc (2004), Particle flow code in 2-dimensions (PFC2D), Version 3.10, Minneapolis, Minnesota, USA.
- Jung, M.C., Hwang, J.S., Kim, J.S., Kim, S.W. and Baek, S.C. (2014), "Influence of the existing cavern on the stability of adjacent tunnel excavation by small-scale model tests," *J. Korean Geo-Environ. Soc.*, **15**(12), 117-128.
- Kang, J.G., Yang, H.S. and Jang, S.J. (2014), "Stability analysis of rock pillar in the diverging area of road tunnel", *J. Korean Tunn. Undergr. Sp. Assoc.*, **24**(5), 344-353.
- Yu, K. and Lu, Z. (2015), "Influence of softening curves on the residual fracture toughness of post-fire normal-strength concrete", *Comput. Concrete*, **15**(2), 102-111. <http://dx.doi.org/10.12989/cac.2015.15.2.199>.
- Khodayar, A. and Nejati, H.R. (2018), "Effect of thermal-induced microcracks on the failure mechanism of rock specimens", *Comput. Concrete*, **22**(1), 93-100. <http://dx.doi.org/10.12989/cac.2018.22.1.093>.
- Kim, J.H. and Kim, J.W. (2017), "Stability estimation of the pillar between twin tunnels considering various site conditions," *J. Korean Tunn. Undergr. Sp. Assoc.*, **27**(2), 109-119.
- Kim, J.K. and Lee, S. (2013), "A study on the estimation of the behaviors by compression method of rock pillar between close parallel tunnels", *J. Korean Geotech. Soc.*, **29**(12), 87-94.
- Kim, J.W. and Bae, W.S. (2008), "A study for the stability investigation of three parallel tunnels using scaled model tests," *J. Korean Tunn. Undergr. Sp. Assoc.*, **18**(4).
- Kim, W.B., Yang, H.S. and Ha, T.H. (2012), "An assessment of rock pillar behavior in very near parallel tunnel", *J. Korean Tunn. Undergr. Sp. Assoc.*, **22**(1), 60-68.
- Kovári, K. (2003), "History of the sprayed concrete lining method—part II: milestones up to the 1960s", *Tunnel. Underground Space Technol.*, **18**(1), 71-83. [https://doi.org/10.1016/S0886-7798\(03\)00006-3](https://doi.org/10.1016/S0886-7798(03)00006-3).
- Li, X.G. and Yuan, D.J. (2012), "Response of a double-decked metro tunnel to shield driving of twin closely under-crossing tunnels", *Tunnel. Underground Space Technol.*, **28**, 18-30. <https://doi.org/10.1016/j.tust.2011.08.005>.
- Li, X., Yan, Z., Wang, Z. and Zhu, H. (2015), "Experimental and analytical study on longitudinal joint opening of concrete segmental lining", *Tunnel. Underground Space Technol.*, **46**, 52-63. <https://doi.org/10.1016/j.tust.2014.11.002>.
- Lim, H.M. and Son, K.R. (2014), "The stability analysis of near parallel tunnels pillar at multi-layered soil with shallow depth by numerical analysis", *J. Korean Geo-Environ. Soc.*, **15**(1), 53-62.
- Liu, H.Y., Small, J.C., Carter, J.P. and Williams, D.J. (2009), "Effects of tunnelling on existing support systems of perpendicularly crossing tunnels", *Comput. Geotechnics*, **36**(5), 880-894. <https://doi.org/10.1016/j.compgeo.2009.01.013>.
- Marji, M.F., Hosseinmorshehy, A. and Shadpour, A. (2008), "On the boundary element analysis of stresses and strains around underground excavations in rocks", *ISRM International Symposium - 5th Asian Rock Mechanics Symposium*, Tehran, Iran, November.
- Monfared, M.M. (2017), "Mode III SIFs for interface cracks in an FGM coating-substrate system", *Struct. Eng. Mech.*, **64**(1), 78-95. <http://dx.doi.org/10.12989/sem.2017.64.1.071>.
- Nabil, B., Abdelkader, B., Miloud, A. and Noureddine, B. (2012), "On the mixed-mode crack propagation in FGMs plates: comparison of different criteria", *Struct. Eng. Mech.*, **61**(3), 201-213. <http://dx.doi.org/10.12989/sem.2017.61.3.371>.
- Nejati, H.R. and Ghazvinian, A. (2014), "Brittleness effect on rock fatigue damage evolution", *Rock Mech. Rock Eng.*, **47**(5), 1839-1848. <https://doi.org/10.1007/s00603-013-0486-4>.
- Pan, B., Gao, Y. and Zhong, Y. (2014), "Theoretical analysis of overlay resisting crack propagation in old cement concrete pavement", *Struct. Eng. Mech.*, **52**(4), 167-181. <http://dx.doi.org/10.12989/sem.2014.52.4.829>.
- Panaghi, K., Golshani, A. and Takemura, T. (2015), "Rock failure assessment based on crack density and anisotropy index variations during triaxial loading tests", *Geomech. Eng.*, **9**, 793-813. <http://dx.doi.org/10.12989/gae.2015.9.6.793>.
- Potyondy, D.O. and Cundall, P.A. (2004), "A bonded-particle model for rock", *Int. J. Rock. Mech. Min. Sci.*, **41**(8), 1329-1364. <https://doi.org/10.1016/j.ijrmms.2004.09.011>.
- Ramadoss, P. and Nagamani, K. (2013), "Stress-strain behavior and toughness of high-performance steel fiber reinforced concrete in compression", *Comput. Concrete*, **11**(2), 55-65. <http://dx.doi.org/10.12989/cac.2013.11.2.149>.
- Rooh, A., Nejati, H. and Goshtasbi, K. (2018), "A new formulation for calculation of longitudinal displacement profile (LDP) on the basis of rock mass quality", *Geomech. Eng.*, **6**(5), 539-545. <https://doi.org/10.12989/gae.2018.16.5.539>.
- Sarfarazi, V. and Haeri, H.A. (2016), "Review of experimental and numerical investigations about crack propagation", *Comput. Concrete*, **18**(2), 235-266. <http://dx.doi.org/10.12989/cac.2016.18.2.235>.
- Shi, J., Ng, C.W.W. and Chen, Y. (2015), "Three-dimensional numerical parametric study of the influence of basement excavation on existing tunnel", *Comput. Geotechnics*, **63**, 146-158. <https://doi.org/10.1016/j.compgeo.2014.09.002>.
- Shin, J.H., Potts, D.M. and Zdravkovic, L. (2005), "The effect of pore-water pressure on NATM tunnel linings in decomposed granite soil", *Canadian Geotechnical J.*, **42**(6), 1585-1599. <https://doi.org/10.1139/t05-072>.
- Siahmansouri, A., Gholamnejad, J. and Marji, M.F. (2012), "A new method to predict ratio of width to height rock pillar in twin circular tunnels", *J. Geol. Geosci.*, **1**, 103. <http://dx.doi.org/10.4172/2329-6755.1000103>.

- Xie, J., Gunn, M.J. and Rahim, A. (2004), "Collapse analysis for two parallel circular tunnels with different diameters in soil" *Proceedings of the Ninth International Symposium on Numerical Models in Geomechanics-NUMOG IX*, Ottawa, Canada, August. 421-426.
- Ye, F., Gou, C. F., Sun, H. D., Liu, Y. P., Xia, Y. X. and Zhou, Z. (2014), "Model test study on effective ratio of segment transverse bending rigidity of shield tunnel", *Tunnel. Underground Space Technol.*, **41**, 193-205. <https://doi.org/10.1016/j.tust.2013.12.011>.
- Zhao, C. (2015), "Analytical solutions for crack initiation on floor-strata interface during mining", *Geomech. Eng.*, **8**, 237-255.

CC